



Spatiotemporal variations in traffic activity and their influence on air pollution levels in communities near highways

Paola Filigrana^{a,*}, Chad Milando^b, Stuart Batterman^b, Jonathan I. Levy^c, Bhramar Mukherjee^d, Sara D. Adar^a

^a Department of Epidemiology, University of Michigan, 1415 Washington Heights, Ann Arbor, MI, 48109-2029, USA

^b Department of Environmental Health Sciences, University of Michigan, 1415 Washington Heights, Ann Arbor, MI, 48109-2029, USA

^c Department of Environmental Health, Boston University, 715 Albany St, T4W, Boston, MA, 02118-2526, USA

^d Department of Biostatistics, University of Michigan, 1415 Washington Heights, Ann Arbor, MI, 48109-2029, USA

HIGHLIGHTS

- Traffic and congestion vary considerably over time and place.
- Few analyses account for this spatiotemporal variation.
- Areas closer to highways had the largest spatiotemporal variations in concentrations.
- In regions with low congestion, AADT data was sufficient to capture pollution patterns.
- In regions with high congestion, resolved data captured greater variation in pollution.

ARTICLE INFO

Keywords:

Traffic-generated air pollution
dispersion model
RLINE
Vehicle emissions
Exposure assessment

ABSTRACT

Localized variations in traffic volume and speed can influence air pollutant emissions and corresponding concentrations in nearby communities, but most studies have utilized only aggregated traffic activity data. In this study, we compared the estimated influence of highway traffic activity on concentrations of primary oxides of nitrogen (NO_x) and fine particulate matter (PM_{2.5}) in communities near highways using a dispersion model informed by highly spatiotemporally-resolved variations of traffic volume and flow compared to the use of Annual Average Daily Traffic (AADT) data at a few locations.

We used two sources of traffic activity data on 500 half-mile roadway segments on the five major highways in the Washington State Puget Sound during 2013. The first consisted of vehicle counts available every half-mile and 5 min; the second was traffic information (e.g., AADT) aggregated across the year and roadway network. Using the Motor Vehicle Emissions Simulator (MOVES) and the Research Line source dispersion model (RLINE), we modeled hourly concentrations of primary NO_x and PM_{2.5} generated by highway traffic at nearly 4000 residences within 1 km of major highways. These concentrations were aggregated to daily and annual average concentrations, which were compared by input data source.

At most locations, concentrations of primary NO_x and PM_{2.5} modeled using the resolved traffic data had similar spatial and temporal distributions to concentrations predicted using the AADT data. However, several areas showed large differences. For example, 25% of residences within 150 m of a highway had concentrations that differed by more than 19% (8 ppb) for NO_x and 32% (0.7 µg/m³) for PM_{2.5}, and the AADT data consistently predicted lower concentrations than the resolved traffic data.

Our findings indicate that temporal and spatial variation in traffic patterns can result in complex spatiotemporal variations of air pollutant concentrations that can be captured with the use of dispersion modeling with the appropriate inputs. The use of spatiotemporally resolved traffic activity data can improve exposure estimates and help reduce exposure measurement error in epidemiological studies, especially in communities near highly congested highways.

* Corresponding author.

E-mail addresses: filigranapaola@gmail.com (P. Filigrana), cmilando@umich.edu (C. Milando), stuartb@umich.edu (S. Batterman), jonlevy@bu.edu (J.I. Levy), bhramar@umich.edu (B. Mukherjee), sadar@umich.edu (S.D. Adar).

<https://doi.org/10.1016/j.atmosenv.2020.117758>

Received 10 April 2020; Received in revised form 2 July 2020; Accepted 3 July 2020

Available online 12 July 2020

1352-2310/© 2020 Elsevier Ltd. All rights reserved.

1. Introduction

Exposure to traffic-related air pollution remains a public health concern due to associations with increased risks of mortality and adverse cardiovascular and respiratory endpoints (Health Effects Institute (HEI), 2010). Concerns are especially evident for communities near major highways given elevated concentrations within hundreds of meters of large roads (Health Effects Institute (HEI), 2010; Zhu et al., 2002). This has important implications given that up to 45% of the United States population in large urban areas lives within 300–500 m of major roads (Health Effects Institute (HEI), 2010; Meyer et al., 2013). Near-road populations also include larger proportions of low-income households and minority racial/ethnic groups (Gunier et al., 2003; Havard et al., 2009; Houston et al., 2004; Meyer et al., 2013; Morello-Frosch et al., 2002; Tian et al., 2012; Wu and Batterman, 2006) that may be more susceptible and vulnerable to effects of pollutant exposure.

Accurately estimating exposures to traffic-related air pollutants is challenging since many factors determine both vehicle emissions and corresponding concentrations (Batterman et al., 2015a; Gokhale, 2011; Kimbrough et al., 2013). A key factor is traffic activity, which can vary considerably over time and place, both within and between highways. For example, traffic can transition from free-flowing to congestion conditions in time and distance scales of minutes and kilometers, respectively. Such variations can influence concentrations of traffic-related pollutants in nearby communities yet have not been routinely incorporated into exposure models for epidemiologic studies given data limitations. Rather, most epidemiologic studies of short-term exposures to traffic-related air pollution have used daily or hourly variation in concentrations measured at air quality monitoring stations (AQS) (Atkinson et al., 2016; Basagaña et al., 2015; Finnbjornsdottir et al., 2015; Grazuleviciene et al., 2004; Tsai et al., 2010). This is likely problematic, however, since monitoring sites in most networks are too sparse to capture the full spatiotemporal variation of traffic-related air pollution in the near-road environments. Land use regression or hybrid models are increasingly able to characterize daily variation utilizing a combination of surface and satellite measurements, and dispersion model outputs, but generally have insufficiently fine resolution for traffic-related primary pollutants (Parvez and Wagstrom, 2019; Son et al., 2018; Wilton et al., 2010).

Vehicle emissions and dispersion models have recently been used in environmental health studies as methods that can overcome many of the challenges of assessing population exposures to traffic-related air pollutants in near road environments (Batterman et al., 2020, 2015b; 2014, 2010; Chang et al., 2015; Isakov et al., 2014; Jerrett et al., 2005; Kanda et al., 2013; Levitin et al., 2005; Patterson and Harley, 2019; Snyder et al., 2014, 2013a; Vette et al., 2013; Zhai et al., 2016; Zhang and Batterman, 2010). These models can predict air pollutants from traffic over a large area with high spatiotemporal resolution by combining emissions from on-road traffic volumes and flow with physical processes in the atmosphere due to meteorology. However, due to a paucity of spatiotemporally resolved traffic data and computational demands, researchers have generally used traffic data aggregated over time and space as inputs to these models. For example, they have used annual average daily traffic (AADT) volumes estimated at a few permanent traffic recorders (PTR), along with regional trends in traffic activity across hours, days, and months and national averages for vehicle speeds (Batterman, 2015; Batterman et al., 2015b, 2014; Chang et al., 2015; Milando and Batterman, 2018a, 2018b; Snyder et al., 2014). Although these approaches help account for temporal variability and have shown improvements in modeling vehicle emissions compared to (unchanging) AADT (Lindhjem et al., 2012), aggregated traffic metrics may not completely capture differences in traffic emissions from localized traffic patterns that vary over time and place.

This research describes the air quality modeling approach we used to estimate exposure to primary oxides of nitrogen (NO_x) and fine particulate matter ($\text{PM}_{2.5}$) generated by highway traffic in support of an

epidemiological study conducted to quantify associations between these pollutants and daily mortality in communities near major highways of the Puget Sound in Washington State, U.S. In this study, we aimed to characterize the influence of variations in highway traffic activity on concentrations of NO_x and $\text{PM}_{2.5}$ generated as primary pollutants (herein referred to as traffic-generated NO_x and $\text{PM}_{2.5}$) at residential locations of all non-accidental mortalities that occurred within 1 km of major highways. We estimated these concentrations using vehicle emissions and a line-source dispersion model with a unique source of traffic data that had finely resolved spatiotemporal variations of traffic volume and speed. We compared these predicted concentrations to those estimated using more typical and aggregated traffic data. We conducted this research in the urban area of the Washington Puget Sound, one of the few regions that has very highly resolved spatiotemporal traffic data.

2. Methods

To predict concentrations of traffic-generated NO_x and $\text{PM}_{2.5}$ from highways in near-road communities, we used two sources of traffic activity data for the main highways in the Puget Sound (i.e., Interstates 5, 405 and 90, and State Routes 167 and 520) during the year of 2013. The first dataset had traffic volume and speed data recorded every half-mile and 5 min (herein referred to as our “resolved traffic data”); the second had traffic volume and speeds aggregated across the year and space (referred to as “AADT data”). These data were incorporated into the Motor Vehicle Emissions Simulator (MOVES, version 2014) (U.S. Environmental Protection Agency, 2014) to generate hourly emission factors (g/vehicle-mile) of primary NO_x and $\text{PM}_{2.5}$ from the Puget Sound highways. We then used the Research Line source dispersion model (RLINE v1.2) (Snyder et al., 2013a) to predict hourly concentrations of traffic-generated NO_x and $\text{PM}_{2.5}$ at residential locations of all non-accidental deaths that occurred within 1 km of a highway between 2009 and 2013. These are intended to represent the exposure distribution of the population and will be informative for our future epidemiological study using this model. Finally, we compared the spatial and temporal distribution of the traffic inputs and predicted concentrations between the two data sources. Below, we describe in more detail the three major components of this modeling framework. Fig. 1 shows the air quality modeling framework.

2.1. Receptor locations

In preparation for our related epidemiological study, we estimated concentrations of traffic-generated NO_x and $\text{PM}_{2.5}$ at the 3784 residential locations of all individuals that died from non-accidental causes within 1 km of our targeted highways between 2009 and 2013. We obtained death certificates with geocoded residential addresses from the Washington Department of Health (WADOH). We also predicted concentrations at regulatory monitoring stations in the Air Quality System (AQS) in the Central Puget Sound that sampled for reactive oxides of nitrogen (NO_y , $n = 1$ monitoring site) as an indicator for NO_x and $\text{PM}_{2.5}$ ($n = 5$, monitoring sites). Fig. 2 displays the receptor locations and the study domain: 9.5% of receptors were within 150 m of the nearest large roadway).

2.2. Traffic data

We obtained spatiotemporally resolved data on traffic volume and vehicle speeds for each half-mile of the highways in the region at 5-min resolution from the Washington State Transportation Center at the University of Washington (TRAC-UW). These five highways are classified as National Functional Classes (NFC) 11 (Urban Interstate) and 12 (Urban Other Freeway or State Routes) and totaled 250 miles in length. Induction loop detectors embedded in the pavement measure real-time traffic volume and vehicle speeds in each direction. These data undergo routine quality assurance screening by the TRAC-UW to ensure

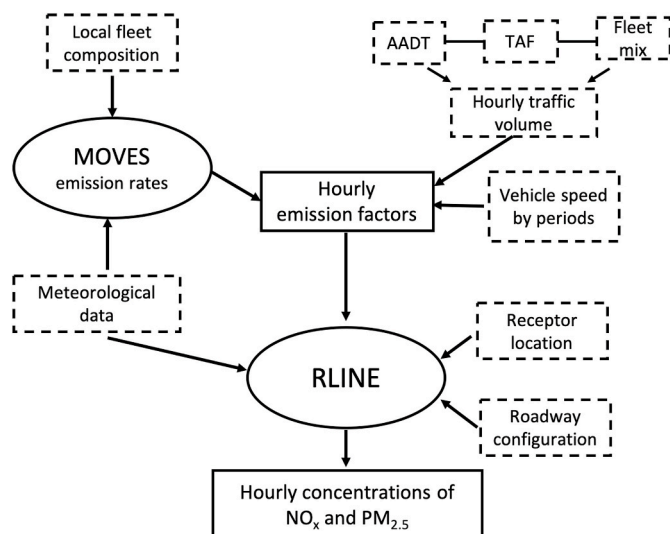


Fig. 1. Flow chart of the air quality modeling framework and input data. Note: The dashed boxes represent input data, the ovals represent computational software and the rectangular elements represent output data. The input data represented in this flow chart corresponds to the AADT data. The main difference with the resolved traffic data is that we used measured hourly traffic volume and vehicle speeds for each half-mile as opposed to the AADT at PTRs, TAF and national vehicle speed used for the AADT data.

high data quality.

For the same roadways, we obtained AADT data from the Washington State Department of Transportation (WSDOT), derived from traffic counts in 2013 at 20 PTRs distributed along the five highways and reported for each direction of the highways (i.e., I-5: six, I-405: five, I-90: three, SR-167: three and SR-520: four). We obtained local temporal allocation factors (TAFs) from the Washington State Department of Ecology that describe general patterns in traffic volumes by month, day of week (weekday and weekend) and hour of day for the region. Due to the absence of aggregated local data for vehicle speeds, these data were obtained from the National Speed Survey for five time periods of the day (i.e., Off-peak-1: 12:00 a.m.-6:59 a.m., morning peak: 7:00 a.m.-8:59 a.m., mid-day: 9:00 a.m.-3:59 p.m., afternoon peak: 4:00 p.m.-6:59 p.m., and off-peak-2: 7:00 p.m.-11:59 p.m.) (De Leonardis et al., 2018).

For both sources of traffic data, we used information on vehicle class from the WSDOT collected at the PTRs and mapped these data to the six Highway Performance Monitoring System (HPMS) classes (i.e., motorcycles, passenger cars, light-duty trucks, buses, single-unit trucks, multi-trailer trucks). We further obtained data from the WSDOT on vehicular age distributions and fuel formulation for King County as inputs to Mobil Vehicle Emissions Simulator model, the emissions simulator, as described below.

For our resolved traffic data, we calculated hourly traffic volumes by vehicle class for each half-mile road segment and direction for all 8760 h of 2013 by weighting our resolved traffic volumes by the vehicle class fractions. For the AADT data, we estimated hourly traffic volume by vehicle class using the AADTs and TAFs for each roadway segment between PTRs by roadway direction.

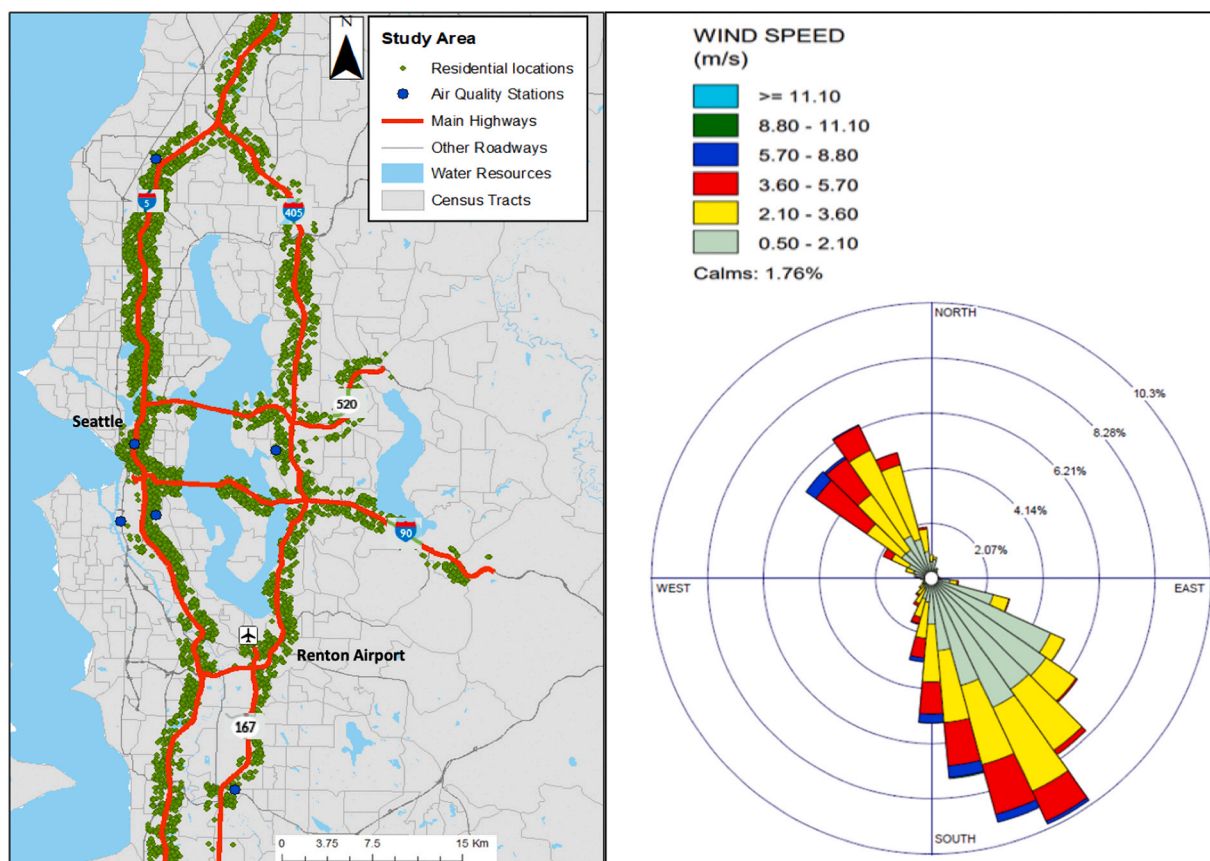


Fig. 2. Study area including major roadways, receptor locations, and prevailing wind direction. in the Central Puget Sound, WA.

Note: Fig. 2 shows the study domain including the five major highways represented as red lines, receptor locations (i.e., 3748) where we predicted concentrations of air pollutants denoted as green dots and the prevailing wind direction at the National Oceanic and Atmospheric Administration (NOAA) station at the Renton Airport. Of the 3748 receptors 9.5% were within 150 m of a highway.

Locational data from the Tiger products of the US Census Bureau were obtained to map the road network of our five targeted highways <https://www2.census.gov/geo/tiger/TIGER2013/ROADS/>.

2.3. Meteorological data

We obtained the hourly meteorological parameters from the Renton airport station operated by the National Oceanic and Atmospheric Administration (NOAA, 2013). These data were processed through the AERMET program by the Puget Sound Clean Air Agency. AERMET estimates boundary layer parameters required for RLINE to model dispersion, including friction velocity (u^*), convective velocity (w^*), surface roughness height (z_0), Monin-Obukhov length (L), moisture, albedo, cloud cover, and temperature. We selected the Renton airport as the primary data source based on its location in our study region and because comparisons of wind profiles measured at other meteorological stations in the region showed similar behavior as that found at the Renton airport.

2.4. On-road mobile vehicle emissions

For both our resolved and AADT input data, we generated hourly vehicle emissions factors (g/vehicle-mile) of NO_x and $\text{PM}_{2.5}$ for each road segment using MOVES-2014 (U.S. Environmental Protection Agency, 2014). Following the approach of Cook et al. (2008) and Snyder et al. (2014), we ran MOVES at the county scale using rate-per-distance calculations of emission rates. We generated emission rates of NO_x and $\text{PM}_{2.5}$ for the running exhaust and evaporative emission processes for the unique combinations of 6 HPMS vehicle types, 16 vehicle speed bins (ranging from 2.5 to 75+ mph), local ambient temperature and relative humidity (every 5 °F), and month. Since running losses during extended idling are not related to highway driving, we did not include this emission process in our calculations (Cook et al., 2008; Snyder et al., 2014). We did, however, include non-exhaust emissions of $\text{PM}_{2.5}$ such as tire wear and brake wear in our models.

To estimate total emissions for each road segment and hour, we integrated the outputs from MOVES with the hourly traffic volume and speed for each vehicle class by road segment based on the month and weather. We performed these calculations for each of the two sources of traffic data described above, resulting in hourly, segment-by-segment emission factors for NO_x and $\text{PM}_{2.5}$ for the resolved and AADT datasets that accounted for local weather and traffic activity in each road segment and direction.

2.5. Dispersion modeling

We ran a modified version of the RLINE dispersion model (v1.2) to predict hourly concentrations of primary NO_x and $\text{PM}_{2.5}$ originating from vehicle emissions on the major highways at our receptor locations. RLINE simulates the dispersion of primary, chemically inert pollutants in near road environments without accounting for chemical transformations or deposition.

The model includes more advanced wind and roadway configuration algorithms providing more advantages of RLINE over previous dispersion models recommended by EPA (Snyder et al., 2013a). Performance evaluations of RLINE have shown good agreement between model estimates and measured air pollutant concentrations (Milando and Bat-terman, 2018a, 2018b; Snyder et al., 2013a). The model also has been recognized as a valid approach to assess air pollutant exposure from traffic emissions in epidemiological studies (Pennington et al., 2018; Zhang et al., 2020).

We implemented RLINE using the numerical integration method with an iteration limit of 1,000, an error limit of 0.001, and the beta algorithms for roadside noise barriers. To avoid running RLINE for each air pollutant, we used the unit emission rate (1 g/m/s) input approach (Snyder et al., 2014) and then scaled hourly RLINE outputs for the

pollutant-specific emission factors from MOVES for each road segment. This assumes that chemical transformations of NO_x and removal processes for $\text{PM}_{2.5}$ have relatively small effects at the spatial scale (<1 km) of our modeling.

A field study showed good agreement between estimates modeled by RLINE and measurements of NO collected at 7 m and 17 m from the roadway shoulder though the model performed better in downwind as compared to upwind estimations. In both cases, however, the model over-predicted as compared to observed concentrations (Snyder et al., 2013b).

2.6. Concentration estimation

We aggregated the modeled hourly concentrations of traffic-generated NO_x and $\text{PM}_{2.5}$ contributed by every road segment in the highway network to each receptor location to obtain 24-h and annual average concentrations. RLINE predictions of NO_x concentrations in $\mu\text{g}/\text{m}^3$ were converted to ppb using the average conversion rate of $1 \mu\text{g}/\text{m}^3 \text{NO}_x = 0.5495 \text{ ppb NO}_x$.

2.7. Data analysis

We characterized the spatial and temporal distributions of traffic volumes and speeds as well as predicted concentrations of NO_x and $\text{PM}_{2.5}$ from highway traffic for the two sources of traffic data using descriptive statistics, Spearman correlation coefficients, box plots, cumulative density function graphics, and heat maps. We also compared the modeled 24-h average concentrations of traffic-generated NO_x and $\text{PM}_{2.5}$ with the measured daily concentrations at AQS monitoring sites. We made comparisons across the two data sources for the entire period of study and by weekdays/weekends and distance to roadway. We also split the variation into a spatial component by evaluating only the annual average concentrations at different locations and a temporal component by focusing on differences in daily concentrations from an annual average. All analyses were conducted using Stata statistical software version 14.1 (Stata Corp) and ArcGIS version 10.1 (ESRI).

3. Results

3.1. Variation in traffic volume and speed on major highways

Table 1 shows some differences in the daily average traffic volumes between the two sources of traffic data, e.g., higher traffic volumes in the resolved traffic data as compared with the AADT data for most regions on all highways except for I-405. We found regions where traffic volumes for the resolved traffic data were greater than 50% (e.g., I-5 and I-90) or twice (e.g., SR-520) the volumes of the AADT data. Traffic volumes were more than 12% and 30% higher on weekdays as compared with Saturdays and Sundays, respectively, and 60% higher during morning and afternoon rush hours as compared to off-peak periods (Table 2).

We also observed substantial spatial variation across road segments within the same roadway, especially for I-5 (Fig. 3 and Supplemental Figure S1, Panels A and B). As expected, the within-highway variation was substantially greater in the resolved traffic data: the AADT volumes in the resolved traffic data were 1.5–3.5 times more variable than the AADT traffic data. As shown in Fig. 3, Panel B and Figure S1, Panel A, most of this variability is driven by the I-5 road segments located in the highly congested area of downtown Seattle, which reached maximum daily average traffic volumes of 450,000 vehicles.

We also found substantial day-to-day variation in traffic volumes in the resolved traffic data, with 60% of road segments reporting between-day standard deviations across weekdays and weekends of over 22,000 and 28,000 vehicles, respectively (Supplemental Figure S1, Panel B). This variation was especially great for the interstate highways. In contrast, for the AADT data, traffic volumes were less temporally

Table 1

Annual average daily traffic volumes (SD) by traffic activity data, highway, PTR and day of week.

| Highway | PTR | AADT data in 1000s of cars/day | | | Resolved data in 1000s of cars/day | | | % Difference for weekdays |
|---------|----------------|--------------------------------|-----------------|-----------------|------------------------------------|-----------------|------------------|---------------------------|
| | | Weekdays | Saturdays | Sundays | Weekdays | Saturdays | Sundays | |
| I-5 | P1 | 185 (12) | 162 (7) | 141 (6) | 187 (24) | 169 (43) | 151 (25) | 1.1 |
| | S189 | 200 (13) | 176 (8) | 152 (6) | 184 (23) | 168 (43) | 153 (25) | 8.3 |
| | P3 | 186 (12) | 163 (7) | 142 (6) | 182 (25) | 163 (42) | 148 (27) | 2.2 |
| | R046 | 208 (13) | 183 (8) | 158 (7) | 236 (54) | 310 (79) | 290 (45) | 12.6 |
| | S202 | 230 (15) | 202 (9) | 175 (7) | 334 (41) | 182 (45) | 168 (28) | 36.9 |
| | S809 | 195 (13) | 172 (8) | 149 (6) | 213 (27) | 182 (47) | 170 (29) | 8.8 |
| | Average | 200 (19) | 176 (14) | 152 (12) | 210 (62) | 186 (71) | 171 (±58) | 4.9 |
| I-405 | S824 | 119 (8) | 105 (5) | 91 (4) | 124 (18) | 107 (27) | 91 (15) | 4.1 |
| | S822 | 192 (12) | 169 (8) | 146 (6) | 186 (28) | 160 (42) | 136 (23) | 3.2 |
| | S204 | 201 (13) | 177 (8) | 153 (7) | 178 (25) | 159 (44) | 138 (26) | 12.1 |
| | D1 | 150 (10) | 132 (6) | 114 (5) | 145 (20) | 132 (34) | 117 (19) | 3.4 |
| | S821 | 155 (10) | 136 (6) | 118 (5) | 148 (21) | 136 (35) | 121 (19) | 4.6 |
| | Average | 175 (26) | 154 (22) | 133 (19) | 148 (32) | 132 (40) | 114 (26) | 16.7 |
| | R017 | 135 (9) | 119 (5) | 103 (4) | 221 (33) | 180 (48) | 166 (29) | 48.3 |
| I-90 | S203 | 148 (10) | 130 (6) | 113 (5) | 154 (22) | 129 (33) | 118 (20) | 4.0 |
| | S825 | 125 (8) | 110 (5) | 95 (4) | 128 (20) | 108 (28) | 98 (17) | 2.4 |
| | Average | 135 (12) | 119 (9) | 103 (8) | 150 (42) | 125 (44) | 115 (33) | 10.5 |
| | P6 | 119 (8) | 105 (5) | 91 (4) | 139 (16) | 134 (10) | 109 (18) | 15.5 |
| SR-167 | R113 | 97 (6) | 85 (4) | 74 (3) | 99 (13) | 89 (8) | 69 (12) | 2.0 |
| | Average | 98 (8) | 86 (6) | 75 (5) | 133 (26) | 121 (23) | 96 (23) | 30.3 |
| SR-520 | S502 | 46 (3) | 40 (2) | 35 (1) | 103 (18) | 66 (22) | 59 (13) | 76.5 |
| | D10 | 63 (4) | 56 (3) | 48 (2) | 111 (18) | 72 (29) | 64 (18) | 55.2 |
| | S533 | 95 (6) | 83 (4) | 72 (3) | 124 (23) | 82 (25) | 71 (16) | 26.5 |
| | S547 | 75 (5) | 66 (3) | 57 (2) | 138 (22) | 98 (28) | 83 (15) | 59.2 |
| | Average | 66 (19) | 58 (16) | 50 (14) | 114 (25) | 76 (28) | 66 (18) | 53.3 |

Note: For the AADT data, the standard deviation (SD) was obtained by applying the TAFs by month, day of week and hour a day to AADT reported at the PTRs throughout the highways. PTRs are located in the following mileposts I-5 (P1: 184.5, S189: 179.5, P3: 176.5, R046: 168.5, S202: 162, S809: 148), I405 (S824: 29, S822: 19, D1: 9, S821: 7), I-90 (R017: 4, S203: 10.5, S825: 14.5), SR-167 (P6: 25, R113: 14.5), SR-520 (S502: 0.5, D10: 4, S533: 8, S547: 12).

Table 2

Hourly average traffic volumes (SD) on weekdays by traffic activity data, highways, and rush hours.

| Highway | AADT data in 1000s of cars/day | | | Resolved data in 1000s of cars/day | | |
|---------|--------------------------------------|--|---------------------------------|--------------------------------------|--|---------------------------------|
| | Morning rush hours (6:00–8:59 am) | Afternoon rush hours (4:00–6:59 pm) | Off-peak (Mid-day and Night) | Morning rush hours (6:00–8:59 am) | Afternoon rush hours (4:00–6:59 pm) | Off-peak (Mid-day and Night) |
| I-5 | 10 (3) | 15 (1) | 7 (4) | 12 (4) | 13 (3) | 8 (5) |
| I-405 | 9 (3) | 13 (2) | 6 (4) | 8 (2) | 9 (2) | 5 (4) |
| I-90 | 7 (2) | 10 (0.9) | 5 (3) | 10 (3) | 10 (3) | 5 (4) |
| SR-167 | 5 (2) | 7 (0.6) | 3 (2) | 7 (2) | 7 (1) | 5 (3) |
| SR-520 | 3 (1) | 5 (1) | 2 (2) | 8 (2) | 8 (2) | 4 (3) |

Note: For the AADT data the standard deviation (SD) was obtained by applying the TAFs by month, day of week and hour a day to AADT reported at the PTRs throughout the highways.

variable, with between-day standard deviations across weekdays and weekends below 14,000 and 13,000 vehicles for all highways, respectively.

Consistent with the volume data, daily average speeds also varied over space and time, and between and within highways (Fig. 3, Panel C). Unlike the volume data, however, this was only evident in the resolved traffic data as there was no (spatial or temporal) variation in the AADT data. Like the volume data, speed was especially variable in the half-mile road segments on I-5 near the Seattle downtown as well as near the SeaTac Airport in Renton south of the I-5/I-405 junction. We also found day-to-day variation in speed for the resolved traffic data, with 60% of road segments with between-day standard deviations across weekdays of over 8 mph (Supplemental Figure S1, Panel C). In contrast, weekend data were less variable (60% of road segments with between-day standard deviations over 4 mph). Speeds in the resolved traffic data also showed the expected pattern of stop-and-go congestion during morning and afternoon peak hours (Supplemental Figure S2). As shown in Figure S3, speeds on the five highways drop from 70 mph to less than 40 mph several times a day.

3.2. Comparison of modeled traffic-generated NO_x and $\text{PM}_{2.5}$ concentrations to measurements

At the AQS monitoring sites, modeled 24-h average concentrations of traffic-generated NO_x slightly exceeded measured concentrations of ambient NO_y (Supplemental Table S1), while modeled concentrations of traffic-generated $\text{PM}_{2.5}$ were only 10–40% of measured concentrations of ambient $\text{PM}_{2.5}$, which represents primary and secondary contributions from both traffic and non-traffic sources. $\text{PM}_{2.5}$ predictions were similar to measured BC concentrations, which is an indicator of traffic-related particulate matter. Modeled concentrations were moderately correlated with measured daily AQS data (R_{sp} for NO_y : 0.5 and $\text{PM}_{2.5}$: 0.3–0.5). (Supplemental Table S1).

3.3. Spatial variation of traffic-generated NO_x and $\text{PM}_{2.5}$ in near-road communities

At the residential receptors, NO_x and $\text{PM}_{2.5}$ concentrations predicted using the resolved traffic data were slightly higher than those using AADT data (Supplemental Table S1), although the spatial distributions were similar, e.g., for annual average concentrations, the R_{sp} for both NO_x and $\text{PM}_{2.5}$ was 0.96. (Supplemental Table S1). As expected,

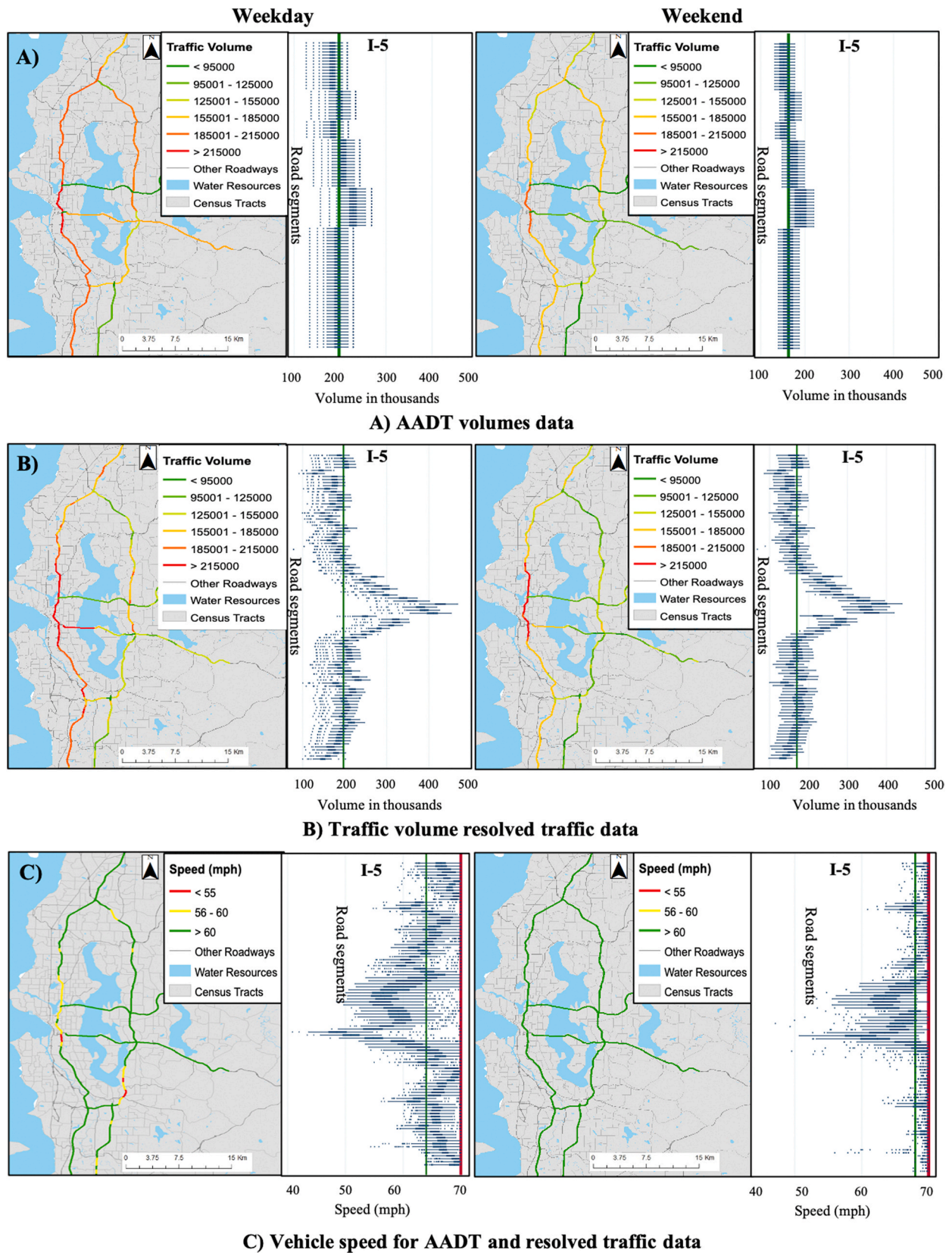


Fig. 3. Spatiotemporal variation of traffic volumes within the AADT (A) and resolved (B) traffic datasets and vehicle speed (C) by day of week and traffic activity data for all roads (maps) and for I-5 (boxplots).

Note: The maps illustrate the mean volume and speed by road segment on all roads for weekdays and weekends separately. The box plots illustrate the within-road segment variability of traffic volumes and speed for all segments along I-5 (north and southbound combined). Mean speed for the AADT data is represented as red line (mean weekday and weekends: 70 mph). Mean speed for resolved traffic data is represented as a green line (mean weekday: 63 mph and mean weekend: 68 mph).

concentrations increased near areas with more traffic and in downwind areas (Fig. 4 and Supplemental Figure S4). Both models predicted higher concentrations at receptors near highways, e.g., the highest concentrations 65 and 72 ppb for NO_x and 3 and 4 $\mu\text{g}/\text{m}^3$ for $\text{PM}_{2.5}$ were obtained within 50 m for the AADT and resolved traffic data, respectively, compared to 30 and 33 ppb for NO_x and 1.8 and 1.6 $\mu\text{g}/\text{m}^3$ for $\text{PM}_{2.5}$ obtained for the AADT and resolved traffic data, respectively beyond 300 m. (Supplemental Figure S5). However, several areas showed large differences, especially those nearest to highly congested road segments and areas with the greatest differences in traffic volumes between the two data sources (Fig. 5 and Supplemental Figure S6). As shown in Fig. 5, we found that 25% of our receptors had differences in concentrations between the two models that were larger than 15% (i.e., 4 ppb) for NO_x and 17% (0.3 $\mu\text{g}/\text{m}^3$) for $\text{PM}_{2.5}$ with the AADT data consistently predicting lower concentrations than models using the resolved traffic data (Supplemental Figure S6 shows results for $\text{PM}_{2.5}$). These differences were greater among near-road receptors (i.e., <150 m) where 25% of the receptors had differences larger than 19% (i.e., 8 ppb) and 32% (i.e., 0.7 $\mu\text{g}/\text{m}^3$) for NO_x and $\text{PM}_{2.5}$, respectively.

Traffic volume showed substantial influence on NO_x concentrations, while vehicle speed showed greater contributions to the variability of $\text{PM}_{2.5}$. For example, we found greater NO_x concentrations for both sets of traffic activity data on receptors close to regions where traffic volumes were the highest (i.e., close to I-5 and I-405 for the resolved and AADT data, respectively) (Fig. 4). These two areas also showed the greatest differences in modeled NO_x concentrations between the two sets of traffic activity data (Fig. 5). In contrast, greater concentrations and greater differences in concentrations of $\text{PM}_{2.5}$ were found on areas with greater variability in vehicle speed such as those close to I-5 and the highly congested area near downtown Seattle (Supplemental Figures S4 and S6).

3.4. Temporal variation of traffic-generated NO_x and $\text{PM}_{2.5}$ in near-road communities

Among all receptor locations, the daily variability of NO_x and $\text{PM}_{2.5}$

concentrations from both models was greatest for receptors within 150 m of highways and near road segments with high traffic variation (Fig. 6 and Supplemental Figure S7). These near-road areas also showed the greatest differences in the temporal variability between the two models, e.g., 25% of receptors within 150 m had differences in the between-day SD that are greater than 19% (6 ppb) for NO_x and 21% (0.7 $\mu\text{g}/\text{m}^3$) for $\text{PM}_{2.5}$ (Fig. 7 and Supplemental Figure S8).

4. Discussion

In this study, we characterized the influence of highway traffic activity on traffic-generated NO_x and $\text{PM}_{2.5}$ concentrations in near-road communities using dispersion modeling and two sources of traffic data. Our results suggest that, in general, AADT and resolved input data produced similar concentrations of traffic-generated NO_x and $\text{PM}_{2.5}$. However, a key finding of our work is that omitting variable traffic volume and speed will lead to increased exposure error, particularly at receptors near major roadways. The magnitude of the difference in predicted concentrations by models was non-trivial. We found the greatest differences in concentrations of both air pollutants between the two models in regions where there were highly variable vehicle density and stop-and-go conditions during rush hours, with models using the AADT data consistently predicting lower concentrations than models using the resolved traffic data. Regions with highly variable traffic flow, such as near the highly-populated area of downtown Seattle, are presumably better captured by the resolved traffic data that has information over very short distances.

In addition, we observed greater differences between the models downwind from roadways, where RLINE is known to better predict concentrations (Snyder et al., 2013b). Factors causing these differences differed somewhat by pollutant: traffic volume was the most substantial contributor to the variability of NO_x concentrations, and vehicle speed for $\text{PM}_{2.5}$ concentrations. Specifically, the availability of variable vehicle speeds with our resolved traffic data allowed us to capture the influence of brake and tire wear emissions characteristic of stop-and-go traffic conditions on $\text{PM}_{2.5}$ concentrations. This differed from the national

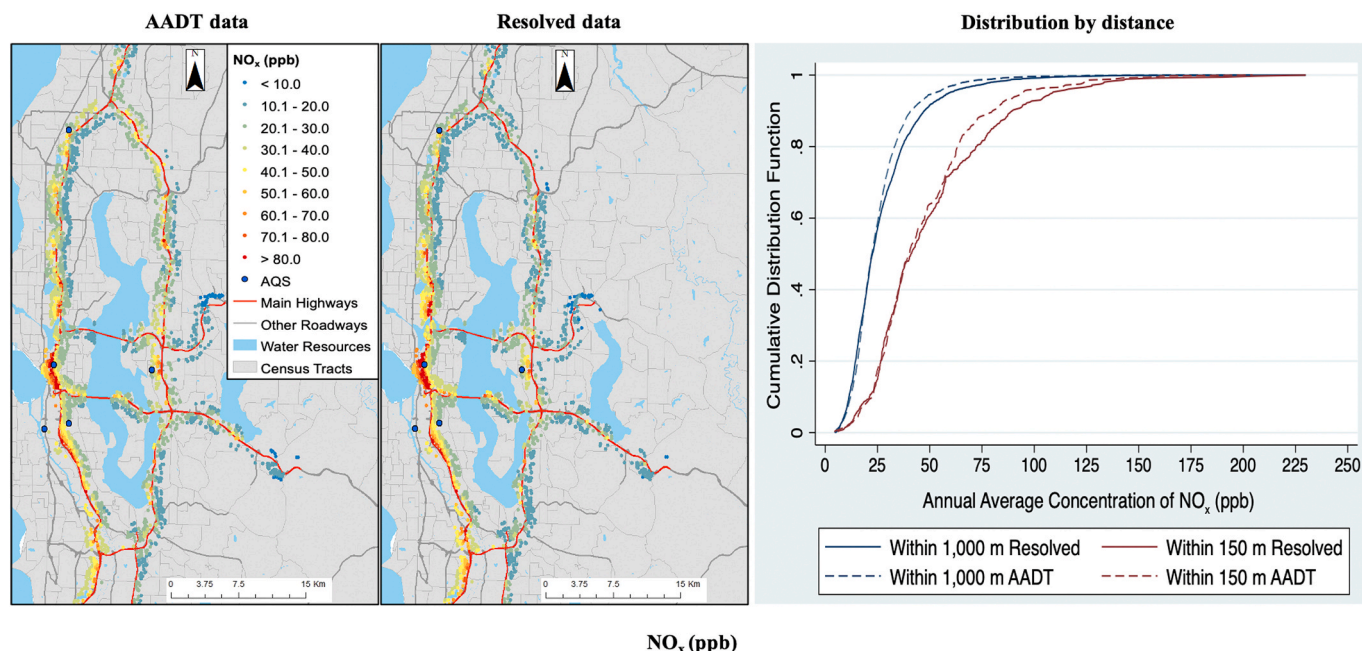


Fig. 4. Spatial distribution of the annual average concentrations of traffic-generated NO_x by traffic activity data.

Note: The heat maps to the left illustrate the annual average concentration of traffic-generated NO_x estimated at each receptor location by traffic input data. The distributions by distance illustrate the cumulative distribution function of concentrations of NO_x by traffic activity data and distance from the highways. The solid lines represent the resolved data and the dash lines represent the AADT data. The blue lines represent concentration at receptors within 1000 m, while the red lines are the concentrations of receptors within 150 m of a highway.

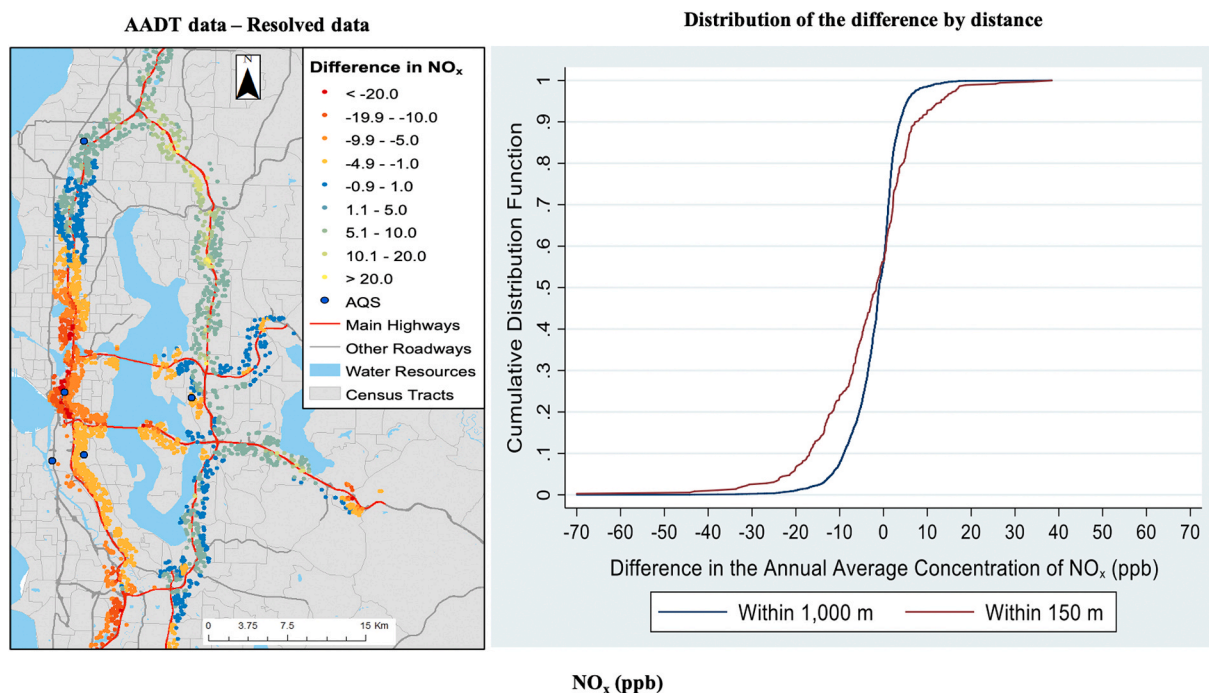


Fig. 5. Distribution of the difference in annual average modeled concentrations of traffic-generated NO_x between models using the two different traffic activity data by distance from the highways.

Note: The heat map illustrates the difference between the two sources of traffic data on the annual average concentration of NO_x at each receptor location. Negative values in the difference in concentrations represent locations where RLINE using the resolved traffic activity data estimated greater concentrations than the AADT data. The cumulative distribution function figures illustrate the distribution of the differences for the annual average concentration between the two sources of data by distance from the highways. Blue lines represent receptors within 1000 m, while red lines represent receptors within 150 m of a highway.

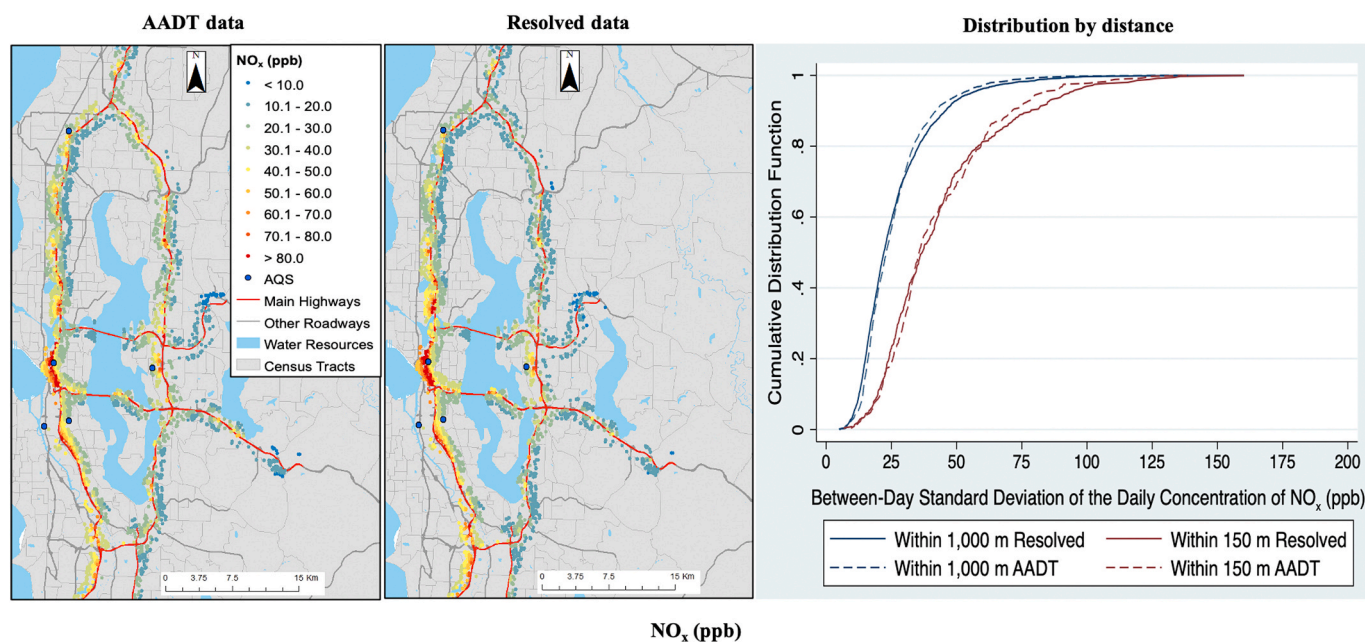


Fig. 6. Spatial distribution of temporal variation (i.e., between-day standard deviations) of the daily concentration of traffic-generated NO_x over the year by traffic activity data.

Note: The heat maps to the left represent the between-day standard deviation of NO_x at each receptor location by traffic input data. The figure of the distribution by distance to the right represents the cumulative distribution function of concentrations by traffic activity data and distance from the highways. The solid lines represent the resolved data and the dash lines represent the AADT data. The blue lines represent concentration at receptors within 1000 m, while the red lines are the concentrations of receptors within 150 m of a highway.

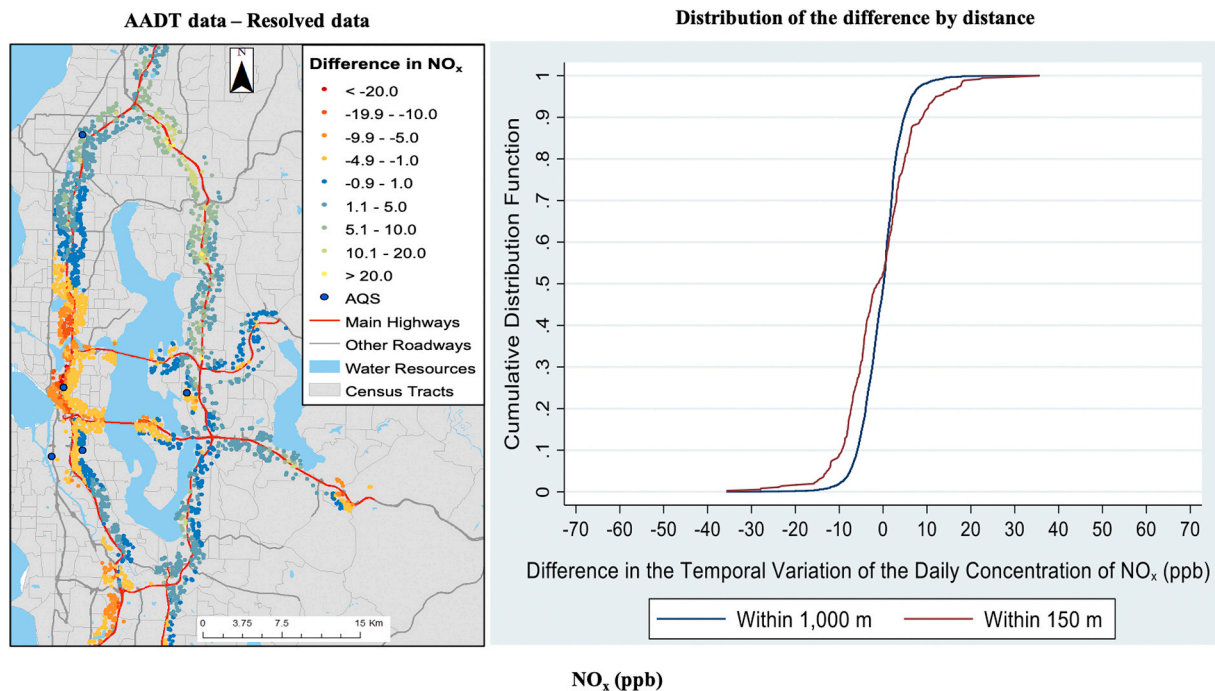


Fig. 7. Distribution of the difference in between-day standard deviations of modeled concentrations of traffic-generated NO_x between models using the two different traffic activity data by distance from the highways.

Note: The heat map illustrates the difference between the two sources of traffic data on the between-day standard deviation of the daily concentrations of NO_x at each receptor location. Negative values in the difference in concentrations represent locations where RLINE using the resolved traffic activity data showed greater standard deviations in concentrations than the AADT data. The cumulative distribution function figures illustrate the distribution of the differences for the temporal variation between the two sources of data by distance from the highways. Blue lines represent receptors within 1000 m, while red lines represent receptors within 150 m of a highway.

speed data, which showed no temporal variation and thus has much smaller predictions from this non-exhaust source (Health Effects Institute (HEI), 2010; Padoan and Amato, 2018; Thorpe and Harrison, 2008). Differences between the data sources due to stop-and-go traffic conditions could be larger than those found in this study since the estimation of brake and tire wear emissions is highly complex and MOVES may underestimate these non-exhaust emissions contributions. Nevertheless, our analysis suggests the importance of traffic activity for NO_x and $\text{PM}_{2.5}$, and future work might explore differences in other pollutants (e.g., metals and polycyclic aromatic hydrocarbons), that might be strongly related to stop-and-go conditions.

Incorporating detailed traffic data did not significantly increase the computational demands in the air quality modeling. For the same number of receptors, there was only a 17% increase in the time of RLINE implementation and post-processing of modeled concentrations with the resolved traffic data. This suggests that the inclusion of detailed spatiotemporal traffic data into dispersion models, when available, may be a worthwhile refinement for some regulatory purposes and epidemiological studies. For example, it may be that using more resolved traffic activity data in the exposure modeling for an epidemiological study of traffic-generated air pollution will increase the variability of exposures and thus the power to detect associations. It may also reduce bias due to exposure measurement error (Sheppard et al., 2012; Szpiro and Paciorek, 2013). This is likely to be especially true for areas with high variations in traffic patterns.

Despite of the strengths of our approach, there are some limitations of this study. First, the ability to use finer resolved traffic data may only apply to major highways with traffic monitoring, a subset of the true roadway system. While this is likely not problematic for receptors near these highways that are the focus of this work, this may be an important omission for receptors further from major highways that might receive the contributions from non-highway roads (i.e., principal and minor arterials). Thus, future work is needed to explore if a similar approach is

possible for the impacts of vehicles on smaller roads. A dense network of traffic recorders (each half-mile in the case study) is unusual and costly, and such information is unavailable in other cities. Despite detailed quality assessment reviews, the resolved traffic data may contain errors, e.g., as shown by differences in traffic volumes for Route 520. Finally, RLINE's performance is known to be sensitive to many factors such as the model input data and assumptions regarding the impact of the local terrain. We cannot confirm the accuracy of our pollution estimates, and RLINE does not account for terrain and complex wind fields that are likely to be present in Seattle. This is in part mitigated by the similarity and correlation between modeled and measured levels of NO_y ; these correlations are within ranges found previously (Milando and Batterman, 2018a). For $\text{PM}_{2.5}$, concentrations and correlations were lower. However, traffic is only one of many sources in urban environments and our predictions are consistent with the expected fraction (~12%) of traffic-generated $\text{PM}_{2.5}$ (Health Effects Institute (HEI), 2010). Lastly, RLINE does not portray atmospheric transformation and deposition (Milando and Batterman, 2018b, 2018a), however, our application emphasized sites within 1 km of roads where these omissions may be less limiting.

5. Conclusion

Temporal and spatial variation in traffic patterns has both regular and aperiodic components that can result in complex spatiotemporal variations of air pollutant concentrations. The use of dispersion modeling with appropriate inputs can capture much of this variation. Concentrations of traffic-related air pollutants predicted using Seattle's unique and comprehensive traffic monitoring dataset had greater temporal and spatial variability than estimates based on aggregated traffic data, particularly near major roads that are frequently congested. The use of spatiotemporally resolved traffic activity data may improve exposure estimates and help reduce exposure measurement error in near

road communities in epidemiological studies.

CRediT authorship contribution statement

Chad Milando: Methodology, Software, Resources, Writing - review & editing. **Stuart Batterman:** Conceptualization, Methodology, Software, Writing - review & editing, Supervision. **Jonathan I. Levy:** Methodology, Writing - review & editing. **Bhramar Mukherjee:** Writing - review & editing. **Sara D. Adar:** Conceptualization, Methodology, Resources, Supervision, Writing - review & editing.

Declaration of competing interest

The authors declare that they have no known competing financial interests or personal relationships that could have appeared to influence the work reported in this paper.

Acknowledgments

The authors acknowledge: Mark Hallenbeck and his team at the University of Washington Transportation Center for providing the resolved traffic volumes and speed data to conduct this research. Washington State Agencies such as the Washington State Department of Transportation and the Air Quality Program of the Washington State Department of Ecology for providing the information to generate the AADT data and data inputs for MOVES. Phil Swartzendruber at the Puget Sound Clean Air Agency for providing AERMET outputs of meteorological conditions in the region. Alex Cao, consultant at the Consultant for Statistics, Computing and Analytics Research of the Rackham Graduate School, University of Michigan for providing assistance and support to processing big datasets.

Appendix A. Supplementary data

Supplementary data to this article can be found online at <https://doi.org/10.1016/j.atmosenv.2020.117758>.

References

- Atkinson, R.W., Analitis, A., Samoli, E., Fuller, G.W., Green, D.C., Mudway, I.S., Anderson, H.R., Kelly, F.J., 2016. Short-term exposure to traffic-related air pollution and daily mortality in London, UK. *J. Expo. Sci. Environ. Epidemiol.* 26, 125–132. <https://doi.org/10.1038/jes.2015.65>.
- Basagaña, X., Jacquemin, Bénédict, Karanasiou, Angeliki, Ostro, Bart, Querol, Xavier, Agis, David, Alessandrini, Ester, Alguacil, Juan, Artinano, Begoña, Catrambone, Maria, De La Rosa, J.D., Díaz, J., Faustini, Annunziata, Ferrari, Silvia, Forastiere, Francesco, Katsouyanni, Klea, Linares, Cristina, Perrino, Cinzia, Ranzi, Andrea, Ricciardelli, I., Samoli, Evangelia, Zauli-Sajani, Stefano, Sunyer, J., Stafoggia, Massimo, Alessandrini, E., Angelini, P., Berti, G., Bisanti, L., Cadum, E., Catrambone, M., Chiusolo, M., Davoli, M., De' Donato, F., Demaria, M., Gandini, M., Grota, M., Faustini, A., Ferrari, S., Forastiere, F., Pandolfi, P., Pelosini, R., Perrino, C., Pietrodangelo, A., Pizzi, L., Poluzzi, V., Priod, G., Randi, G., Ranzi, A., Rowinski, M., Scarinzi, C., Stafoggia, M., Stivanello, E., Zauli-Sajani, S., Dimakopoulou, K., Eleftheriadis, K., Katsouyanni, K., Kelessis, A., Maggos, T., Michalopoulos, N., Pateraki, S., Petrakakis, M., Rodopoulou, S., Samoli, E., Sytsa, V., Agis, D., Alguacil, J., Artinano, B., Barrera-Gómez, J., De La Rosa, J., Díaz, J., Fernandez, R., Jacquemin, B., Karanasiou, A., Linares, C., Ostro, B., Perez, N., Pey, J., Querol, X., Salvador, P., Sanchez, A.M., Tobias, A., Bidondo, M., Declercq, C., Le Tertre, A., Lozano, P., Medina, S., Pascal, L., Pascal, M., 2015. Short-term effects of particulate matter constituents on daily hospitalizations and mortality in five South-European cities: results from the MED-PARTICLES project. *Environ. Int.* 75, 151–158. <https://doi.org/10.1016/j.envint.2014.11.011>.
- Batterman, S., 2015. Temporal and spatial variation in allocating annual traffic activity across an urban region and implications for air quality assessments. *Transport. Res. Transport Environ.* 41, 401–415. <https://doi.org/10.1016/j.trd.2015.10.009>.
- Batterman, S. a, Zhang, K., Kononowech, R., 2010. Prediction and analysis of near-road concentrations using a reduced-form emission/dispersion model. *Environ. Health* 9, 29. <https://doi.org/10.1186/1476-069X-9-29>.
- Batterman, S., Berrocal, V.J., Milando, C., Gilani, O., Arunachalam, S., Zhang, K.M., 2020. HEI, 2020. Enhancing Models and Measurements of Traffic-Related Air Pollutants for Health Studies Using Dispersion Modeling and Bayesian Data Fusion. Research Report 202, Boston, MA.
- Batterman, S., Burke, J., Isakov, V., Lewis, T., Mukherjee, B., Robins, T., 2014. A comparison of exposure metrics for traffic-related air pollutants: application to epidemiology studies in Detroit, Michigan. *Int. J. Environ. Res. Publ. Health* 11, 9553–9577. <https://doi.org/10.3390/ijerph110909553>.
- Batterman, S., Cook, R., Justin, T., 2015a. Temporal variation of traffic on highways and the development of accurate temporal allocation factors for air pollution analyses. *Atmos. Environ.* 107, 351–363. <https://doi.org/10.1016/j.atmosenv.2015.02.047>.
- Batterman, S., Ganguly, R., Harbin, P., 2015b. High resolution spatial and temporal mapping of traffic-related air pollutants. *Int. J. Environ. Res. Publ. Health* 12, 3646–3666. <https://doi.org/10.3390/ijerph120403646>.
- Chang, S.Y., Vizuete, W., Valencia, A., Naess, B., Isakov, V., Palma, T., Breen, M., Arunachalam, S., 2015. A modeling framework for characterizing near-road air pollutant concentration at community scales. *Sci. Total Environ.* 538, 905–921. <https://doi.org/10.1016/j.scitotenv.2015.06.139>.
- Cook, R., Isakov, V., Touma, J.S., Benjey, W., Thurman, J., Kinee, E., Ensley, D., 2008. Resolving local-scale emissions for modeling air quality near roadways. *J. Air Waste Manag. Assoc.* 58, 451–461. <https://doi.org/10.3155/1047-3289.58.3.451>.
- De Leonardis, D., Huey, R., Green, J., 2018. National Traffic Speeds Survey III: 2015 (Report No. DOT HS 812 485). Traffic Tech, Washington, DC.
- Finnbjornsdottir, R.G., Oudin, A., Elvarsson, B.T., Gislason, T., Rafnsson, V., 2015. Hydrogen sulfide and traffic-related air pollutants in association with increased mortality a case-crossover study in Reykjavik, Iceland. *BMJ Open* 5. <https://doi.org/10.1136/bmjopen-2014-007272>.
- Gokhale, S., 2011. Traffic flow pattern and meteorology at two distinct urban junctions with impacts on air quality. *Atmos. Environ.* 45, 1830–1840. <https://doi.org/10.1016/j.atmosenv.2011.01.015>.
- Grazuleviciene, R., Maroziene, L., Dulskiene, V., Malinauskiene, V., Azaraviciene, A., Laurinaviciene, D., Jankauskiene, K., 2004. Exposure to urban nitrogen dioxide pollution and the risk of myocardial infarction. *Scand. J. Work. Environ. Health* 30, 293–298. <https://doi.org/10.5271/sjweh.797>.
- Gunier, R.B., Hertz, A., Von Behren, J., Reynolds, P., 2003. Traffic density in California: socioeconomic and ethnic differences among potentially exposed children. *J. Expo. Anal. Environ. Epidemiol.* 13, 240–246. <https://doi.org/10.1038/sj.jea.7500276>.
- Havard, S., Deguen, S., Zmirou-Navier, D., Schillinger, C., Bard, D., 2009. Traffic-related air pollution and socioeconomic status. *Epidemiology* 20, 223–230. <https://doi.org/10.1097/EDE.0b013e31819464e1>.
- Health Effects Institute (HEI), 2010. HEI Panel on the Health Effects of Traffic-Related Air Pollution. 2010. Traffic-. In: Related Air Pollution: A Critical Review of the Literature on Emissions, Exposure, and Health Effects, vol. 17. HEI Special Report, Boston, MA.
- Houston, D., Wu, J., Ong, P., Winer, A., 2004. Structural disparities of urban traffic in Southern California: implications for vehicle-related air pollution exposure in minority and high-poverty neighborhoods. *J. Urban Aff.* 26, 565–592. <https://doi.org/10.1111/j.0735-2166.2004.00215.x>.
- Isakov, V., Arunachalam, S., Batterman, S., Berezicki, S., Burke, J., Dionisio, K., Garcia, V., Heist, D., Perry, S., Snyder, M., Vette, A., 2014. Air quality modeling in support of the near-road exposures and effects of urban air pollutants study (NEXUS). *Int. J. Environ. Res. Publ. Health* 11, 8777–8793. <https://doi.org/10.3390/ijerph110908777>.
- Jerrett, M., Arain, A., Kanaroglou, P., Beckerman, B., Potoglou, D., Sahuvaroglu, T., Morrison, J., Giovis, C., 2005. A review and evaluation of intraurban air pollution exposure models. *J. Expo. Anal. Environ. Epidemiol.* 15, 185–204. <https://doi.org/10.1038/sj.jea.7500388>.
- Kanda, I., Ohara, T., Nataami, T., Nitta, H., Tamura, K., Hasegawa, S., Shima, M., Nakai, S., Sakamoto, K., Yokota, H., 2013. Development of outdoor exposure model of traffic-related air pollution for epidemiologic research in Japan. *J. Expo. Sci. Environ. Epidemiol.* 23, 487–497. <https://doi.org/10.1038/jes.2013.29>.
- Kimbrough, S., Baldauf, R.W., Hagler, G.S.W., Shores, R.C., Mitchell, W., Whitaker, D.A., Croghan, C.W., Vallero, D.A., 2013. Long-term continuous measurement of near-road air pollution in Las Vegas: seasonal variability in traffic emissions impact on local air quality. *Air Qual. Atmos. Heal.* 6, 295–305. <https://doi.org/10.1007/s11869-012-0171-x>.
- Levitin, J., Härkönen, J., Kukkonen, J., Nikmo, J., 2005. Evaluation of the CALINE4 and CAR-FMI models against measurements near a major road. *Atmos. Environ.* 39, 4439–4452. <https://doi.org/10.1016/j.atmosenv.2005.03.046>.
- Lindhjem, C.E., Pollack, A.K., DenBleyker, A., Shaw, S.L., 2012. Effects of improved spatial and temporal modeling of on-road vehicle emissions. *J. Air Waste Manag. Assoc.* 62, 471–484. <https://doi.org/10.1080/10962247.2012.658955>.
- Meyer, P. a, Yoon, P.W., Kaufmann, R.B., 2013. Center for disease control and prevention. Health disparities and inequalities report - United States, 2013. Residential proximity to mayor highways, United States, 2010. *MMWR. Surveill. Summ.* 62, 3–5.
- Milando, C.W., Batterman, S.A., 2018a. Operational evaluation of the RLIN dispersion model for studies of traffic-related air pollutants. *Atmos. Environ.* 182, 213–224. <https://doi.org/10.1016/j.atmosenv.2018.03.030>.
- Milando, C.W., Batterman, S.A., 2018b. Sensitivity analysis of the near-road dispersion model RLIN - an evaluation at Detroit, Michigan. *Atmos. Environ.* 181, 135–144. <https://doi.org/10.1016/j.atmosenv.2018.03.009>.
- Morello-Frosch, R., Pastor, M., Porras, C., Sadd, J., 2002. Environmental justice and regional inequality in Southern California: implications for future research. *Environ. Health Perspect.* 110, 149–154.
- NOAA, 2013. National Oceanic and Atmospheric Administration data. <https://www.ftp.nce.noaa.gov/pub/data/noaa>, 2013 (accessed 3.9.15).
- Padoan, E., Amato, F., 2018. Vehicle non-exhaust emissions: impact on air quality. In: Amato, F. (Ed.), Non-Exhaust Emissions: An Urban Air Quality Problem for Public Health; Impact and Mitigation Measures. Elsevier Inc., Barcelona, Spain, pp. 21–65. <https://doi.org/10.1016/B978-0-12-811770-5.00002-9>.

- Parvez, F., Wagstrom, K., 2019. A hybrid modeling framework to estimate pollutant concentrations and exposures in near road environments. *Sci. Total Environ.* 663, 144–153. <https://doi.org/10.1016/j.scitotenv.2019.01.218>.
- Patterson, R.F., Harley, R.A., 2019. Evaluating near-roadway concentrations of diesel-related air pollution using RLINE. *Atmos. Environ.* 199, 244–251. <https://doi.org/10.1016/j.atmosenv.2018.11.016>.
- Pennington, A.F., Strickland, M.J., Klein, M., Zhai, X., Bates, J.T., Drews-Botsch, C., Hansen, C., Russell, A.G., Tolbert, P.E., Darrow, L.A., 2018. Exposure to mobile source air pollution in early-life and childhood asthma incidence: the kaiser air pollution and pediatric asthma study. *Epidemiology* 29, 22–30. <https://doi.org/10.1097/EDE.0000000000000754>.
- Sheppard, L., Burnett, R.T., Szpiro, A. a, Kim, S.-Y., Jerrett, M., Pope, C.A., Brunekreef, B., 2012. Confounding and exposure measurement error in air pollution epidemiology. *Air Qual. Atmos. Health* 5, 203–216. <https://doi.org/10.1007/s11869-011-0140-9>.
- Snyder, M., Arunachalam, S., Isakov, V., Talgo, K., Naess, B., Valencia, A., Omary, M., Davis, N., Cook, R., Hanna, A., 2014. Creating locally-resolved mobile-source emissions inputs for air quality modeling in support of an exposure study in detroit, Michigan, USA. *Int. J. Environ. Res. Publ. Health* 11, 12739–12766. <https://doi.org/10.3390/ijerph111212739>.
- Snyder, M.G., Venkatram, A., Heist, D.K., Perry, S.G., Petersen, W.B., Isakov, V., 2013a. RLINE: a line source dispersion model for near-surface releases. *Atmos. Environ.* 77, 748–756. <https://doi.org/10.1016/j.atmosenv.2013.05.074>.
- Snyder, M.G., Venkatram, A., Heist, D.K., Perry, S.G., Petersen, W.B., Isakov, V., 2013b. RLINE: a line source dispersion model for near-surface releases. *Atmos. Environ.* 77, 748–756. <https://doi.org/10.1016/j.atmosenv.2013.05.074>.
- Son, Y., Osornio-Vargas, Á.R., O'Neill, M.S., Hystad, P., Texcalac-Sangrador, J.L., Ohman-Strickland, P., Meng, Q., Schwander, S., 2018. Land use regression models to assess air pollution exposure in Mexico City using finer spatial and temporal input parameters. *Sci. Total Environ.* 639, 40–48. <https://doi.org/10.1016/j.scitotenv.2018.05.144>.
- Szpiro, A.a., Paciorek, C.J., 2013. Measurement error in two-stage analyses, with application to air pollution epidemiology. *Environmetrics* 24, 501–517. <https://doi.org/10.1002/env.2233>.
- Thorpe, A., Harrison, R.M., 2008. Sources and properties of non-exhaust particulate matter from road traffic: a review. *Sci. Total Environ.* 400, 270–282. <https://doi.org/10.1016/j.scitotenv.2008.06.007>.
- Tian, N., Xue, J., Barzyk, T.M., 2012. Evaluating socioeconomic and racial differences in traffic-related metrics in the United States using a GIS approach. *J. Expo. Sci. Environ. Epidemiol.* <https://doi.org/10.1038/jes.2012.83>.
- Tsai, D.H., Wang, J.L., Chuang, K.J., Chan, C.C., 2010. Traffic-related air pollution and cardiovascular mortality in central Taiwan. *Sci. Total Environ.* 408, 1818–1823. <https://doi.org/10.1016/j.scitotenv.2010.01.044>.
- U.S Environmental Protection Agency, 2014. Motor vehicle emission simulator (MOVES): user guide for MOVES2014. EPA-420-B-14-055, July 2014) [WWW Document]. URL: <https://www.epa.gov/moves/moves-versions-limited-current-use#user-2014>.
- Vette, A., Burke, J., Norris, G., Landis, M., Batterman, S., Breen, M., Isakov, V., Lewis, T., Gilmour, M.L., Kamal, A., Hammond, D., Vedantham, R., Berezniccki, S., Tian, N., Croghan, C., 2013. The near-road exposures and effects of urban air pollutants study (NEXUS): study design and methods. *Sci. Total Environ.* 448, 38–47. <https://doi.org/10.1016/j.scitotenv.2012.10.072>.
- Wilton, D., Szpiro, A., Gould, T., Larson, T., 2010. Improving spatial concentration estimates for nitrogen oxides using a hybrid meteorological dispersion/land use regression model in Los Angeles, CA and Seattle, WA. *Sci. Total Environ.* 408, 1120–1130. <https://doi.org/10.1016/j.scitotenv.2009.11.033>.
- Wu, Y.-C., Batterman, S. a, 2006. Proximity of schools in Detroit, Michigan to automobile and truck traffic. *J. Expo. Sci. Environ. Epidemiol.* 16, 457–470. <https://doi.org/10.1038/sj.jes.7500484>.
- Zhai, X., Russell, A.G., Sampath, P., Mulholland, J.A., Kim, B.U., Kim, Y., D'Onofrio, D., 2016. Calibrating R-LINE model results with observational data to develop annual mobile source air pollutant fields at fine spatial resolution: application in Atlanta. *Atmos. Environ.* 147, 446–457. <https://doi.org/10.1016/j.atmosenv.2016.10.015>.
- Zhang, K., Batterman, S., 2010. Near-road air pollutant concentrations of CO and PM2.5: a comparison of MOBILE6.2/CALINE4 and generalized additive models. *Atmos. Environ.* 44, 1740–1748. <https://doi.org/10.1016/j.atmosenv.2010.02.008>.
- Zhang, X., Zhao, H., Chow, W.H., Bixby, M., Durand, C., Markham, C., Zhang, K., 2020. Population-based study of traffic-related air pollution and obesity in Mexican Americans. *Obesity* 28, 412–420. <https://doi.org/10.1002/oby.22697>.
- Zhu, Y., Hinds, W.C., Kim, S., Sioutas, C., 2002. Concentration and size distribution of ultrafine particles near a major highway. *J. Air Waste Manag. Assoc.* 52, 1032–1042. <https://doi.org/10.1080/10473289.2002.10470842>.